THE AMERICAN MINERALOGIST

JOURNAL OF THE MINERALOGICAL SOCIETY OF AMERICA

Vol. 46 JULY–AUGUST, 1961 Nos. 7 and 8

THE REACTION SERIES, GIBBSITE→CHI ALUMINA →KAPPA ALUMINA→CORUNDUM*

G. W. BRINDLEY AND J. O. CHOE, *Department of Ceramic Technology, The Pennsylvania State University, University Park, Pennsylvania.*

ABSTRACT

The reactions of micron-sized powders of gibbsite heated in air progressively to 1350° C. are followed by single crystal electron diffraction patterns, *x*-ray powder patterns, thermogravimetric measurements, infra-red absorption spectrometry and differential thermal analysis. The reaction series gibbsite→χ-Al_2O_3→K-Al_2O_3→corundum is confirmed, with χ-Al_2O_3 in the range 270°–870° C. At about 270° C., the product still retains 25% 'water' which is lost progressively up to about 800° C. From about 970–1180° C., K-Al_2O_3 is present together with α-Al_2O_3. The product termed K- is probably a mixture, since ν-Al_2O_3 and ξ'-Al_2O_3 have also been observed. Analysis of the diffraction data leads to the conclusion that χ- has probably a close-packed hexagonal type structure with $a=5.57$, $c=8.64$ Å, $c/a=1.551$. The principal component of 'κ-' has a large hexagonal cell, with $a=16.7$ Å. The continuity of crystallographic orientations in these reactions is clearly demonstrated by the electron diffraction diagrams.

INTRODUCTION

The thermal reactions of gibbsite

The work of de Boer and his colleagues (1954a, b, 1956), of Tertian and Papée (1958), and of other investigators has shown that the thermal reactions of gibbsite are dependent on many variables, and in particular on the crystal size of the gibbsite, on the atmosphere, and on the rate of heating. Prior to the realization of the importance of these variables, the results were conflicting and poorly understood.

In the present work, fine crystal size, normal atmospheres and slow heating rates are employed. For crystals finer than about 1 micron, it is considered by Tertian and Papée (1958), de Boer, Fortuin, Steggerda (1954*a*, *b*), and others, that the following reactions take place:

$$\text{Gibbsite} \rightarrow \chi\text{-}Al_2O_3 \rightarrow \kappa\text{-}Al_2O_3 \rightarrow \alpha\text{-}Al_2O_3 \qquad \text{(Series I)}$$

For coarse-grained gibbsite, as Brown, Clark and Elliott (1953) first clearly recognized, boehmite is the first product to be formed as a result

* Contribution No. 60-1 from the College of Mineral Industries, The Pennsylvania State University, University Park, Pa.

of the development of a hydrothermal condition in the gibbsite crystals. Subsequently a fissuring of the crystals occurs and the remaining gibbsite then follows reaction series I. The boehmite independently gives rise to a second reaction series, so that two parallel series of reactions take place.

$$\text{Gibbsite} \rightarrow \text{Boehmite} \rightarrow \gamma\text{-}Al_2O_3 \rightarrow \theta\text{-}Al_2O_3 \rightarrow \alpha\text{-}Al_2O_3 \qquad \text{(Series II)}$$

$$\searrow\ \chi\text{-}Al_2O_3 \longrightarrow \kappa\text{-}Al_2O_3 \rightarrow \alpha\text{-}Al_2O_3 \qquad \text{(Series I)}$$

Crystallographic aspects of the reactions

Ervin (1952) emphasized the concept of structural continuity in relation to the numerous intermediate products formed when gibbsite and other hydrated aluminas are converted to the final stable α-alumina, corundum. His arguments were based principally on the continuity of certain dominant reflections in the x-ray powder diagrams. Much earlier, Deflandre (1932) had shown that diaspore transforms to corundum by a crystallographically ordered process, without intermediate products. This reaction takes place at a relatively low temperature, 450–600° C. The sequence of crystallographic changes, gibbsite→boehmite→γ-Al_2O_3 →θ-Al_2O_3, exhibited by coarse gibbsite has been studied by single crystal techniques by Saalfeld (1958, 1959), who has demonstrated the following dimensional relationships:

a(gibbsite)	→	a(boehmite)	→	$[1\bar{1}0]_{\gamma\text{-}Al_2O_3}$	→	$a, \theta\text{-}Al_2O_3$
2.88		2.86		2.81		2.81

The crystallographic relations between the phases or products formed from fine-grained ($<1\mu$) gibbsite have not been analyzed previously, largely because the fine-grained nature of the material precludes the use of single-crystal x-ray analysis, and the x-ray powder data show mainly broad and ill-defined reflections. Tertian and Papée (1958) especially have attempted to clarify the particular features characterizing the χ- and κ-Al_2O_3 which have been designated as the principal intermediate stages in the reaction series of fine-grained gibbsite.

Present Studies

The present studies have been aimed at elucidating in more detail the reaction series I for fine-grained gibbsite heated under normal atmospheric conditions. For this purpose, electron diffraction (E.D.) analysis, which can be applied to single crystals of micron dimensions, has major advantages over x-ray powder studies. It is also necessary to follow in detail the removal of 'water' from the structure, and for this purpose differential thermal analysis, thermo-gravimetric measurements and infra-red absorption measurements have been made.

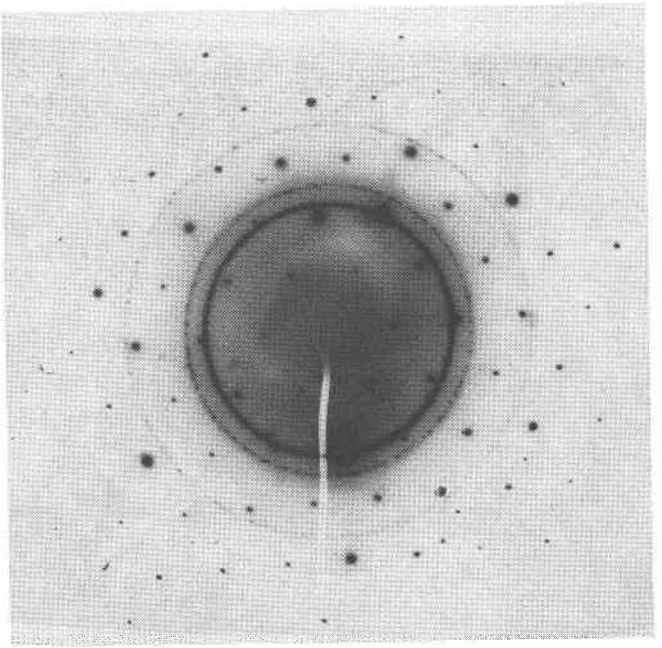

FIG. 1. Electron diffraction pattern of a single crystal of gibbsite "shadowed" with aluminum metal.

Electron-diffraction procedures

Single crystal diagrams were obtained by using well-dispersed samples and an R.C.A. instrument, Type EMU, with a diaphragm for isolating single crystals in the field of view. Spacing calibration of the single-crystal diffraction patterns was obtained by lightly shadowing the samples with metallic aluminum which gave ring patterns of the metal. Fig. 1 shows a typical single crystal spot pattern with superposed calibration rings.

Specimen preparation

Suitable fine-grained gibbsite is essential for these studies. A fine-grained material with particle size <1 micron supplied by the Reynolds Metals Company gave a clear x-ray powder diagram of gibbsite, but proved unsuitable for E.D. study; the particles were shaped so that they took up random orientations in the E.D. camera. By grinding under water a coarse 'platy' gibbsite supplied by the Aluminum Company of America, thin platy crystals of sub-micron size were obtained, which were separated from coarser material by sedimentation in water at a con-

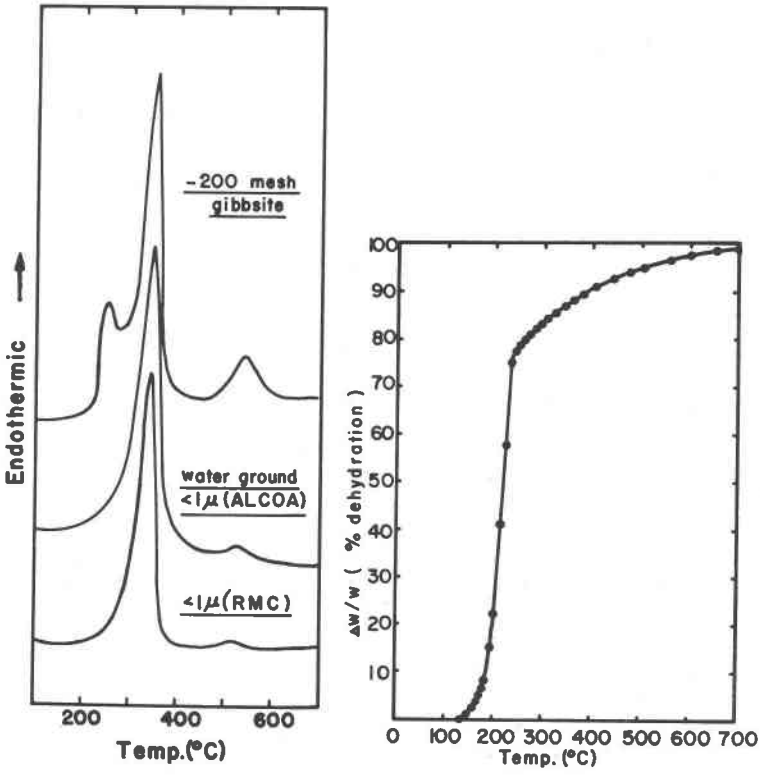

FIG. 2. (Left) Differential thermal analysis curves of (i) −200 mesh gibbsite ("Alcoa"), (ii) sample (i) water-ground to less than 1μ particle size, (iii) gibbsite, 1μ particle size (Reynolds Metals Co.).

FIG. 3 (Right) Progressive weight-loss/temperature curve for <1μ gibbsite; 12 hr. heat-treatment at each temperature.

trolled pH of 6.8–7.2. These crystals were well oriented in the diffraction instrument and gave good E.D. patterns (see Fig. 1).

Following heat-treatment, the products were stored in sealed tubes over P_2O_5. Preparation of specimens for electron microscope and diffraction study was carried out using amyl acetate as the dispersion medium. Fine gibbsite crystals, oriented on a glass plate, were covered by a thin collodion film, and subsequently by a more substantial Formvar film. The combined film was stripped from the glass with the aid of Scotch tape and immersed in ethylene chloride. The Formvar film is dissolved and the thin collodion film with gibbsite attached is caught on grids for insertion in the microscope.

Dehydration studies

Whereas reaction series I is characterized by essentially the single endothermic dehydration reaction, series II is characterized by two dehydration processes. Therefore 'fine' gibbsite is differentiated from 'coarse' gibbsite by having one endotherm rather than three endotherms (see Fig. 2). However, the slow loss of water after an initial rapid loss can be followed more precisely by thermo-gravimetric measurements, and also (though less quantitatively) by infra-red absorption measurements.

Therefore all these techniques have been applied to obtain an understanding of the lower temperature reactions in which 'water' is involved.

X-ray powder measurements

These have been made with a Philips Norelco diffractometer adapted so that a stream of dry air passed over the sample during the recording of data.

Experimental Results

Differential thermal analysis data

Figure 2 shows curves obtained with relatively coarse gibbsite supplied by the Aluminum Company of America, micron-sized gibbsite obtained by grinding the 'ALCOA' material, and micron-sized gibbsite supplied by the Reynolds Metals Company.

The micron-sized powders show traces of an endotherm at about 500° C. which may arise from a small amount of boehmite. However, the more prominent boehmite peak at about 250° C. is not observed from the fine-grained materials.

X-ray powder analysis shows that only a trace of boehmite is formed from the micron-sized powders, and this small amount does not affect adversely the interpretation of the results. Boehmite was not detected in the E.D. diagrams, despite the fact that its pattern is quite distinct from the other patterns observed in these experiments.

Thermo-gravimetric data

Step-wise temperature increments of the order of 5–10° C. at 12 hr. intervals gave the dehydration curve shown in Fig. 3, where $(\Delta w/w_0)$ represents weight loss as a fraction of total weight loss. Dehydration proceeds rapidly in the temperature interval 190–240° C. up to about 75%, and thereafter goes very slowly to completion at about 800° C.

Isothermal dehydration curves show similar features. Sample size is important, as was shown previously for kaolinite and halloysite by

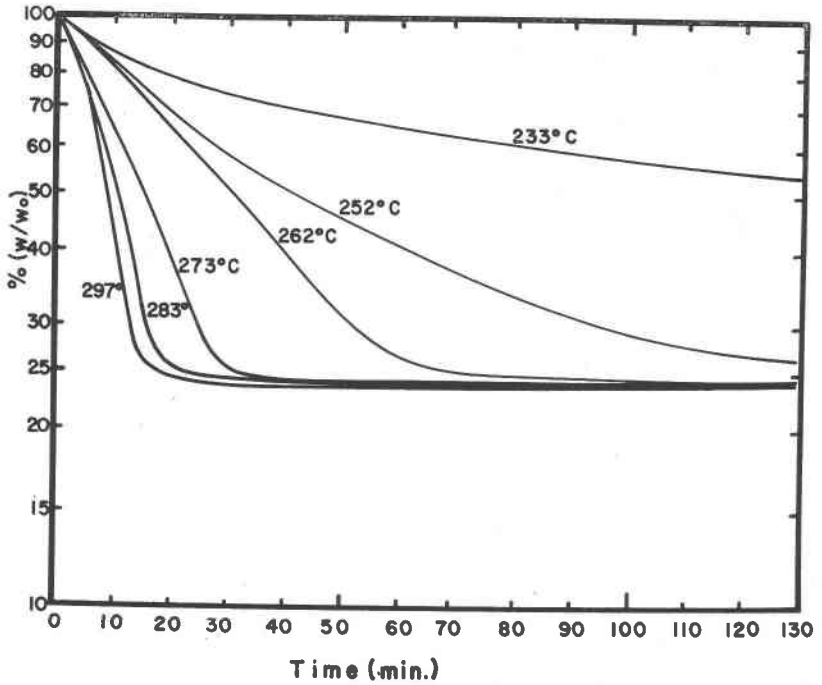

FIG. 4. Isothermal dehydration curves for $<1\mu$ gibbsite.

Brindley and Nakahira (1959). Figure 4 shows typical curves for (w/w_0), where w is the weight of unreacted material, plotted logarithmically against time for thin powder layers heated isothermally at various temperatures. The initial parts of these curves are not strictly linear, so that the reaction proceeds only approximately according to first-order kinetics. When the reactions are about 75% complete, in all cases the reaction rate is reduced almost to zero at the temperatures employed.

Single crystal, electron diffraction data

Figure 5(A–F) shows a series of diagrams illustrating the various spot patterns which have been observed, together with the aluminum calibration rings, for samples heated to various stages of reaction between room temperature and 1180° C. All the patterns are hexagonal in character and exhibit certain features which are constant or nearly constant throughout the reaction series. Hexagonal axes a_1^* and a_2^* are shown in each diagram corresponding to the smallest unit cell compatible with the data.

Table 1 lists the hexagonal parameters, a_H, calculated from the various

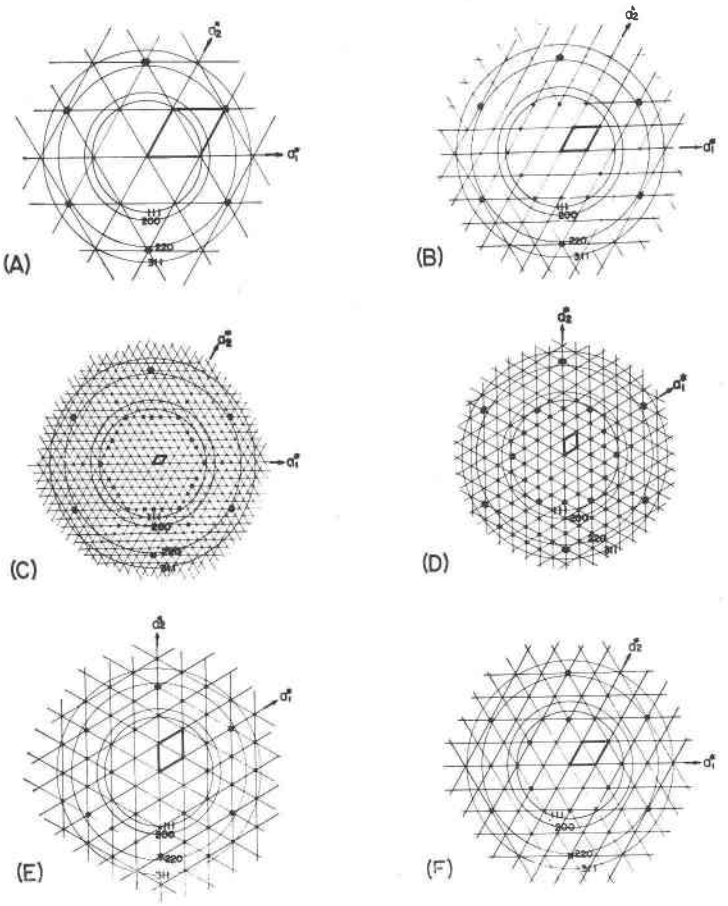

FIG. 5. Single-crystal electron diffraction patterns, with aluminum calibration rings, for transition aluminas.

(A) χ-Al_2O_3 at 270° C.; approximate formula, Al_2O_3 0.75 H_2O; $a_H = 2.77$ Å
(B) χ-Al_2O_3 at 830° C.; formula Al_2O_3; $a_H = 5.53$ Å
(C) κ(?)-Al_2O_3 at 970–1180° C.; $a_H = 16.78$ Å
(D) (?)-Al_2O_3 at 1030–1180° C.; $a_H = 9.70$ Å
(E) ξ'-Al_2O_3 at 1180–1350° C.; $a_H = 5.37$ Å
(F) υ-Al_2O_3 at 1030–1180° C.; $a_H = 5.54$ Å

E.D. patterns. The smallest cell, $a_H = 2.77$ Å (Figure 5A), is obtained on heating at 270° C., with about 75% bulk dehydration. This parameter is about 4% smaller than the corresponding value for gibbsite, namely a(monoclinic)/3 = 2.87 Å. Continued heating and dehydration produces only small changes in the E.D. patterns up to 830° C., when dehydration is virtually complete. At this stage, illustrated by Fig. 5B, weak addi-

TABLE 1. VALUES OF HEXAGONAL PARAMETER, a_H, FOR HEATED ALUMINAS DERIVED FROM FINE-GRAINED GIBBSITE

Temperature, ° C.	Probable designation	E.D. pattern	Parameter, Å	
270	χ (initial)	Fig. 5A		$a_H=1.77$
830	χ (final)	Fig. 5B	$a_H=5.53$	$a/2=2.76_5$
970–1180	κ (?)	Fig. 5C	$a_H=16.78$	$a/6=2.79$
1130–1180	—	Fig. 5D	$a_H=9.70$	$a/(4 \sin 60)=2.80$
1030–1180	ν	Fig. 5F	$a_H=5.54$	$a/2=2.77$
1180–1350	ξ'	Fig. 5E	$a_H=5.37$	$a/2=2.69$
>1000	α	—		

tional spots are observed corresponding with $a_H=5.53$ Å, or $a_H/2=2.76_5$ Å. Some reorganization of the structure, probably of the cations, and a slight contraction have occurred.

In the temperature interval 860–1180° C., further reorganization of the structure takes place with the emergence of reflections on a finer scale in the E.D. diagrams, Figs. 5C and D, corresponding to larger unit cells which, however, are related in a simple way to the original parameters.

At temperatures in the range 1030–1350° C., patterns are occasionally found (Figs. 5E, F) agreeing closely with E.D. patterns described by Cowley (1953) which he labelled ξ'-alumina ($a=5.23$ Å) and ν-alumina ($a=5.53$ Å). These patterns are simpler than those obtained in the temperature range 860–1180° C. X-ray patterns show that α-Al_2O_3 forms at temperatures of about 1000° C., but satisfactory E.D. patterns of the final stage were not obtained, probably owing to sintering of the material.

A statistical survey of the results observed after various heat-treatments is given in Table 2, from which it appears that the principal stages in the reaction series are as follows: From 270–870° C., E.D. patterns

TABLE 2. SINGLE-CRYSTAL E.D. PATTERNS OF TRANSITION ALUMINAS OBSERVED AT VARIOUS TEMPERATURES

Temperature, °C.	Number and type of pattern observed
270°	37 patterns, Fig. 5A
470°	9 patterns, Fig. 5A
830–875°	52 patterns, Fig. 5B
970°	7 patterns, Fig. 5B; 24 patterns, Fig. 5C
1030°	21 patterns, Fig. 5C; 2 patterns, Fig. 5D; 2 patterns, Fig. 5F
1180°	9 patterns, Fig. 5C; 2 patterns, Fig. 5D; 2 patterns, Fig. 5E; 2 patterns, Fig. 5F
1350°	5 patterns, Fig. 5E

of the type shown in Figs. 5A, B are obtained and these may correspond with the material usually labelled χ-Al_2O_3. This result agrees broadly with the conclusion of Tertian and Papée (1958) who gave 200–400° C. up to 900° C. as the temperature range for χ-Al_2O_3. In the temperature range 950–1180° C. more complex patterns are obtained, with Fig. 5C mainly occurring. This material may correspond with κ-Al_2O_3. At 1000° C. and higher temperatures, α-Al_2O_3 (corundum) is formed but satisfactory E.D. patterns of this phase were not obtained.

Rare occurrences of ν- and ξ'-alumina (Figures 5E, F) were found in the temperature range 1030–1350° C.

X-ray powder data

Following the disappearance of gibbsite at about 200–220° C., the *x*-ray powder diagrams are mainly diffuse until α-Al_2O_3 makes its appearance at about 1000° C. From about 270–800° C., the diagram resembles mainly that of χ-Al_2O_3 as described by Tertian and Papée (1958). At 270° C., slight traces of the strongest boehmite reflections can be detected as stated earlier. At 470° C., the diagram appears to be solely that of χ-Al_2O_3, and no further changes occur until about 830° C., when additional broad reflections are observed which may be attributed to κ-Al_2O_3. As the temperature approaches 1000° C., the reflections become clearer, but the development of α-Al_2O_3 at this temperature hinders the analysis of the κ-Al_2O_3. At 970° and higher temperatures, the E.D. patterns have shown that more than one crystalline form develops so that considerable caution is required in the interpretation of *x*-ray powder patterns.

An important result obtained from *x*-ray powder data is that when the intensity of the very strong (002) gibbsite reflection at $d=4.85$ Å, is plotted against percentage dehydration of the sample, the intensity falls smoothly and rapidly to zero at 75% dehydration (See Fig. 6). If the remaining 25% of unreacted material were present as undecomposed gibbsite, it would be very easily detected by *x*-rays. The intensity of the (002) gibbsite reflection is such that a few per cent of gibbsite could be detected easily. The conclusion seems inescapable that about 25% of the initial 'water' content is associated with the first reaction product formed from the gibbsite. This agrees exactly with the composition $Al_2O_3 \cdot 0.75\ H_2O$ given previously by Papée and Tertian (1955).

The *x*-ray powder data obtained from material heated at 470° C., which is believed to be χ-Al_2O_3, are given in Table 3, together with corresponding data by Tertian and Papée (1958), and by Stumpf *et al.* (1950) as amended by Russell *et al.* (1956). The agreement is as good as can be expected for such poorly crystalline material.

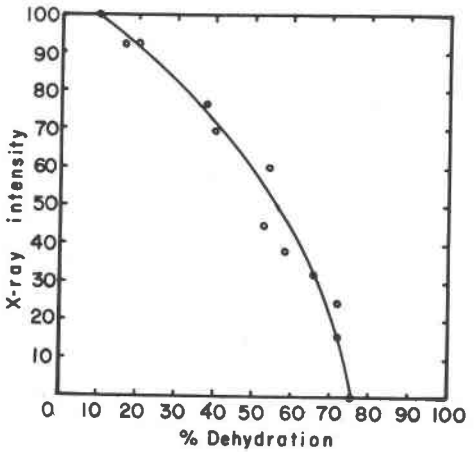

FIG. 6. *X*-ray intensity of (002) gibbsite vs. percentage bulk dehydration.

Infra-red absorption data

Absorption spectra were recorded for representative samples from the various heat-treatments, and the following are the main results achieved. Material heated at 270° C. no longer shows the sharp absorption peaks in the 9.5–15μ range obtained with gibbsite and the strong hydroxyl absorption in the neighborhood of 2.9μ is considerably reduced. The latter is reduced still further at 470° C. and is eliminated at 830° C. The results are consistent with progressive removal of 'water' from about 25% of the initial amount at 270° C. to complete removal by about 800° C.

TABLE 3. DIFFRACTION DATA FOR χ-ALUMINA

d=spacings, in Å (I)=estimated intensity

Tertian & Papée (1958) d(I) (500° C.)	Russell *et al.* (1956) d(I)	Present data 470° C.			
		d(I), observed		calculated	
		X-ray	E.D.	$(hk, l)_H$	d
—	—	4.80±0.15 (4)	—	100	4.822
2.848 (8)	—	2.88±0.02 (8)	—	003	2.880
—	—	—	2.794	110	2.785
2.404 (15)	2.40 (4)	2.41±0.01 (15)	2.401	200	2.411
—	2.27 (2)	—	—		
2.126 (15)	2.11 (3)	2.12±0.01 (15)	—	202	2.106
—	1.98 (2)	1.96±0.01 (10)	—	104	1.971
1.91 (5)	—	—			
—	1.53 (1)	—			
1.394 (35)	1.39 (10)	1.395±0.005 (30)	1.397	220	1.393

Discussion

Electron diffraction data

The group of six strong reflections lying near the Al(220) ring is a constant and important feature of the E.D. patterns of the transition aluminas. The lattice spacing corresponding to these reflections is about 1.395 Å. *X*-ray powder studies have shown a consistently strong reflection at 1.39–1.40 Å (cf. Rooksby (1951); Ervin (1952); Russell *et al.* (1956)). Gibbsite (see Fig. 1) also gives a similar reflection with $d=1.451$ Å.

Ervin (1952) pointed out that this spacing corresponds to the oxygen ion radius in a cubic close-packed system of oxygen ions, and is the spacing of the (440) planes of the spinel structure. This observation is important because the γ- and η-forms are considered to have a spinel-type structure. The reflection is particularly strong because all octahedral and tetrahedral cation sites lie in the (440) planes of the oxygen anions, and therefore the intensity of the reflection is independent of the particular distribution of cations in these sites. However, quite apart from this particular type of structure, one can say that a strong reflection at about $d=1.395$ Å will arise from planes of the type (220) from cubic close-packed oxygen arrangements.

It is equally important to observe that a similar situation exists with hexagonal close-packing. The oxygen anions lie wholly in the $(11\bar{2}0)$ planes, the spacing of which is the oxygen ion radius, and also all the octahedral and tetrahedral cation sites lie in the $(11\bar{2}0)$ planes of anions.

Therefore, while the existence of a strong reflection at $d\simeq 1.395$ is evidence for close-packing of oxygen ions with the aluminum ions in interstitial sites, it does not differentiate between the hexagonal and cubic arrangements.

Indexing of electron diffraction patterns

Care is needed in drawing conclusions from the hexagonal spot patterns given by electron diffraction. Gibbsite provides a warning since this is a monoclinic structure.

Hexagonal diffraction patterns do not exclude cubic structures, because in hexagonal-to-cubic transformations, the plane $(0001)_H$ is likely to become $(111)_C$ with $[111]_C$ replacing $[001]_H$. Any rhombohedral lattice (including as a special case the cubic lattice with $[111]_C$ as the trigonal axis) can be referred to hexagonal axes with the following index relations:

$$\begin{aligned} h_C &= h_H + l_H/3 \\ k_C &= k_H + l_H/3 \\ l_C &= -h_H - k_H + l_H/3 \end{aligned}$$

A cubic structure oriented with $[111]_C$ parallel to the electron beam gives a zero-order reciprocal array satisfying the relation

$$h_C + k_C + l_C = 0$$

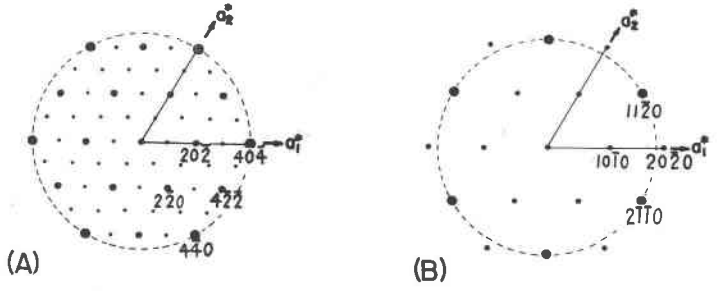

FIG. 7. Zero-level reciprocal lattice diagrams for (A) cubic lattice with respect to [111] axis, and (B) hexagonal close-packed lattice. In (A), small dots refer to simple lattice, large dots to face-centered lattice; cubic indices are given.

or, the cubic indices will be of the type $(h, k, \overline{h+k})_C$. In the zero-level of the hexagonal reciprocal lattice, $l_H=0$ and therefore $h_H=h_C$, $k_H=k_C$, and $(\overline{h+k})_H=l_C$. In other words, zero-level reflections assigned indices $(h, k, \overline{h+k}, 0)_H$ with respect to hexagonal axes, may also have the indices $(h, k, \overline{h+k})_C$ with respect to cubic axes.

Reflections from a *simple* cubic lattice satisfying the relation $h_C+k_C+l_C=0$ are as follows:

$$(1\bar{1}0),\ (11\bar{2}),\ (2\bar{2}0),\ (12\bar{3}),\ (3\bar{3}0),\ (22\bar{4}),\ (13\bar{4}),\ (4\bar{4}0)\cdots$$

For a *face-centered* cubic lattice, which corresponds to cubic close-packing, only the following reflections occur:

$$(2\bar{2}0),\ (22\bar{4}),\ (4\bar{4}0)\cdots$$

Figure 7A shows these two sets of reflections referred to hexagonal axes, with the face-centered cubic reflections emphasized and with the strong reflections of type $(4\bar{4}0)$ strongly emphasized.

Figure 7B shows the zero-order array of reflections to be expected from an hexagonal close-packed system with the strong $(11\bar{2}0)$ reflections strongly emphasized in the diagram.

It is evident that the close-packed cubic and close-packed hexagonal arrangements give rise to similar E.D. patterns in the projection considered here, but the very strong reflections corresponding to planes with $d=r$ (anion) lie *on* the a_1^*, a_2^*, axes in Figure 7A, and *between* these axes in Figure 7B.

Comparison of observed and calculated E.D. patterns

Figure 5A for material heated to 270° C. corresponds exactly with Fig. 7B and it may be inferred that the gibbsite has transformed into an hexagonally close-packed arrangement of oxygen anions.

Figure 5A gives place to diagrams of the type shown in Fig. 5B at about

800° C., having weak, additional spots requiring the hexagonal net to be drawn on half the scale on Fig. 5A. It is inferred that the structure is still essentially hexagonally close-packed with the aluminum ions taking up preferential positions which require a doubling of the hexagonal a parameters.

As the temperature approaches 1000° C., the E.D. patterns remain hexagonal, but become more complex. The pattern most commonly seen is that of Fig. 5C, in which the axes have the same directions as in Figs. 5A and 5B, but the parameters are changed by a factor of 6 with respect to Fig. 5A.

In Figs. 5D and 5E, which occur much less frequently, the strong reflections at about $d = 1.39$–1.40 now lie *on* the a_1^*, a_2^* axes and to this extent correspond with Fig. 7A, but the indices are of the type $(6\bar{6}0)$ in Fig. 5D and $(3\bar{3}0)$ in Fig. 5E, and do not correspond with $(2\bar{2}0)$ or $(4\bar{4}0)$ as would be expected for cubic close-packing.

In Fig. 5F, which occurs rarely in material heated to 1180° C., the axes are oriented as in Figs. 5A, B, and C, but the pattern is simpler than in 5C; it approximates to 5B found at lower temperatures, but with more and better defined reflections.

Indexing and unit cell parameters for χ-Al_2O_3

Table 3 lists the present observed E.D. and x-ray data for χ-Al_2O_3. These have been indexed graphically on the basis of an hexagonal cell, using the indices obtained from the E.D. patterns. The following lattice parameters are obtained:

$$a = 5.57 \text{ Å} \qquad c = 8.64 \text{ A}, \qquad c/a = 1.551.$$

The axial ratio is somewhat less than the ideal value for hexagonal close-packing, 1.632, and suggests a contraction of the structure parallel to c due to the interstitial aluminum ions.

The hexagonal indices and the calculated d-values are listed in Table 3; the observed and calculated spacings are in satisfactory agreement.

The persistence of 'water' to high temperatures

The marked retardation of the dehydration reaction when about 75% complete has been observed by previous investigators (cf. Papée and Tertian, 1955). The thermo-gravimetric and the infra-red data show that the remaining 25% of 'water' is lost gradually over the temperature range from 270–800° C. In rapid heating, as in thermal analysis, the slight endothermic effect observed around 500° C. may be connected in part with this retained water. Although there are traces of boehmite formed from the fine-grained gibbsite, these traces are insufficient to produce the first boehmite endotherm (see Fig. 2).

The absence of any significant change in the E.D. and x-ray patterns between 270° and about 800° C. suggests that the structure remains essentially constant in type, although the crystallinity is obviously very poorly developed. At 830° C., when the dehydration is complete, there is an additional set of spots in the E.D. pattern which can be considered indicative of a more ordered arrangement of the Al cations. The progressive release of the water apparently does not make the structure sufficiently unstable until the temperature reaches 800° C., or thereabouts, and the 'recrystallization' (if it can be so described) still does not alter the main structural pattern which is set by the hexagonal close-packing of the anions. The 'recrystallization' probably takes the form of a re-distribution of Al ions giving a lattice parameter six times as large as that set by the oxygen ions alone.

This recalls the persistence of water in metakaolin discussed in some detail by Stubičan (1959), although the amount is much less than in χ-Al_2O_3 which might almost be described as a 'meta-gibbsite.'

Conclusions

The investigation is concerned with the thermal reactions of submicron sized gibbsite, which are confirmed to be different from those of coarser-sized gibbsite.

The disappearance of the x-ray and electron diffraction patterns of gibbsite when the material is about 75% dehydrated provides strong evidence for the retention of appreciable 'water,' probably hydroxyl ions, in the first reaction product, χ-Al_2O_3. This 'water' is lost gradually in the temperature range 270–800° C., but the diffraction patterns show little change. The diffraction data are interpreted in terms of a close-packed hexagonal type arrangement of oxygen anions, with $a=5.57$ Å, $c=8.64$ Å. $c/a=1.551$.

Continuity of the structural changes occurring in the transition aluminas is shown clearly by the electron diffraction diagrams. At 970° C., a more complex structure with a large hexagonal cell, $a=16.78$ Å, is observed which may be the form designated κ-Al_2O_3. Above this temperature α-alumina (corundum) forms, but during its formation, from 970–1180° C., other transition aluminas are recorded, in particular the forms ξ' and ν previously found by Cowley. Therefore it is believed that powder data must be interpreted with considerable caution.

Acknowledgments

This study forms part of a program on high-temperature reactions supported by a grant (G-5799) to one of us (G.W.B.) from the National Science Foundation.

J. O. Choe wishes to thank the International Cooperation Administration, Washington, D. C., for a travel grant to the U.S.A., and also the National Industrial Research Institute, Seoul, Korea, for leave of absence.

Thanks are due also to the Aluminum Company of America, and the Reynolds Metals Company for materials used in these studies.

References

Boer, J. H. de, Fortuin, J. M. H., and Steggerda, J. J. (1954a), The dehydration of alumina hydrates, *Proc. Kon. Ned. Akad. Wetensch., Amsterdam*, **B.57,** 170–180.

Boer, J. H. de, Fortuin, J. M. H., and Steggerda, J. J. (1954)b, The dehydration of alumina hydrates, II, *Proc. Kon. Ned. Akad. Wetensch., Amsterdam*, **B.57,** 434–444.

Boer, J. H. de, Steggerda, J. J., and Zwietering, P. (1956), The dehydration of alumina hydrates III. *Proc. Kon. Ned. Akad. Wetensch., Amsterdam*, **B.59,** 434–444.

Brindley, G. W., and Nakahira, M. (1957), Kinetics of dehydroxylation of kaolinite and halloysite, *J. Am. Ceram. Soc.*, **40,** 346–350.

Brown, J. F., Clark, D., and Elliott, W. W. (1953), The thermal decomposition of alumina trihydrate, gibbsite, *J. Chem. Soc.*, 84–88.

Cowley, J. M. (1953), Structure analysis of single crystals by electron diffraction. III. Modifications of alumina, *Acta Cryst.*, **6,** 846–853.

Deflandre, M. (1932), La structure cristalline du diaspore, *Bull. Soc. Franç. Min.*, **55,** 140–165.

Ervin, G. (1952), Structural interpretation of the diaspore-corundum and boehmite-γ-Al_2O_3 transitions, *Acta Cryst.*, **5,** 103–108.

Papée, D. and Tertian, R. (1955), Etude de la decomposition thermique de l'hydrargillite et de la constitution de l'alumine activée, *Bull. Soc. Chim. France*, 983–991.

Rooksby, H. P. (1951), Oxides and hydroxides of aluminium and iron, Chapter 10 of "X-Ray Identification and Crystal Structures of Clay Minerals," G. W. Brindley (Editor), Mineralogical Society, London.

Russell, A. S., *et al.* (1956), "Alumina Properties," Technical paper No. 10 (revised), Aluminum Co. of America, Pittsburgh, Pa.

Saalfeld, H. (1958), The dehydration of gibbsite and the structure of a tetragonal γ-Al_3O_3 *Clay Min. Bull.*, **3,** 249–257.

Saalfeld, H. (1959), Einkristalluntersuchungen zum Problem der Hydrargillit-Entwässerung, *Z. Krist.*, **112,** 88–96.

Stubičan, V. (1959), Residual hydroxyl groups in the metakaolin range, *Miner. Mag.*, **32,** 38–52.

Stumpf, H. C., *et al.* (1950), Thermal transformations of aluminas and alumina hydrates, *Ind. Eng. Chem.*, **42,** 1398–1403.

Tertian, R. and Papée, D. (1958), Transformations thermiques et hydrothermiques de l'alumine, *J. Chim. Phys.*, 341–353.

Manuscript received July 13, 1960.

Note added in press: Since this work was completed, a further contribution by H. Saalfeld has appeared (N. Jb. Miner., Abh., 95, 1–87, June 1960) which also discusses the χ-κ reaction series. His results and those reported here agree in some respects, but not in others.